
Article:
Fisher, A.J., Harrison, M.T., Hyatt, N.C. et al. (2 more authors) (2020) The dissolution of simulant UK Ca/Zn-modified nuclear waste glass : insight into Stage III behavior. MRS Advances, 5 (3-4). pp. 103-109. ISSN 2059-8521

https://doi.org/10.1557/adv.2020.50

MRS Advances

The dissolution of simulant UK Ca/Zn-modified nuclear waste glass: Insight into Stage III behaviour

Adam J. Fisher[1], Mike T. Harrison[2], Neil C. Hyatt[1], Russell J. Hand[1] and Claire L. Corkhill[1]

[1]*NucleUS Immobilisation Science Laboratory, Department of Materials Science and Engineering, The University of Sheffield, S1 3JD, UK*

[2]*National Nuclear Laboratory, Central Laboratory, Sellafield, Seascale, Cumbria, CA20 1PG, UK*

ABSTRACT

The dissolution of the United Kingdom's vitrified high-level-waste simulant, CaZn MW28, was investigated following the Product Consistency Test-B protocol for 112 d at 90 °C and in ultra-high-quality water. Residual rate dissolution (stage II) and rate resumption (stage III), after 28 d, was observed. Thermodynamic modelling suggested that solutions were saturated with respect to Mg- and Zn-bearing phases, and the presence of Mg- and Zn-smectite clays was tentatively observed. The formation of these phases was concurrent with a significant increase in the dissolution rate, similar to Stage III behaviour seen in other nuclear waste simulant glass materials, indicating that the addition of Mg and Zn to high-level-waste glass (7.3 wt. % combined) significantly influences the dissolution rate.

INTRODUCTION

The current treatment strategy for high-level-waste (HLW) vitrification in the UK utilises a modified borosilicate base glass, which incorporates Al_2O_3, ZnO and CaO into the traditional Mixed Windscale (MW) glass formulation. With a nominal composition (in wt. %) of $4.2Li_2O{\cdot}8.6Na_2O{\cdot}6.1CaO{\cdot}5.9ZnO{\cdot}4.2Al_2O_3{\cdot}23.4B_2O_3{\cdot}47.6SiO_2$, this glass is referred to as CaZn MW. The transition to CaZn MW is ongoing, with the aims of: (i) incorporating higher quantities of Mo (through the crystallisation of $CaMoO_4$) arising

from post operational clean out (POCO) of the high-activity-liquor storage tanks [1], (ii) reducing the melt viscosity, thereby inducing better melt homogenization and increased levels of waste loading at lower processing temperatures, thus, (iii) enhancing the melter durability, and, (iv) improving the chemical durability in geological disposal environments [2,3].

Controversy surrounds the chemical durability of Zn and Ca containing glass, whereby Zn addition has been reported to increase the chemical resistance to dissolution at the forward rate (Stage I - hydrolysis of the glass network) [4], but has a negative impact at later reaction progress, causing aggressive residual stage II dissolution due to the precipitation of secondary Zn-containing phases [5] or possibly triggering rate resumption (stage III), related to the formation of zeolites [6]. The effect of Ca is generally positive, increasing the chemical resistance to dissolution at the residual rate (stage II) due to strengthening the altered gel network [7-10], but has been shown to encourage stage III due to the formation of calcium silicate phases [11]. These issues are important considerations for predictive models and performance assessments for geological disposal.

At present, CaZn MW is deployed on one out of three active vitrification lines at the Sellafield Ltd. site, incorporating 28 wt. % oxide (o) and Magnox (m) blend waste. Although studies have given insight into the chemical durability of CaZn MW28 [1,12], this study expands on the literature by providing insight into the mechanisms controlling the dissolution of CaZn MW28 at greater reaction progress using the accelerated product-consistency-test B (PCT-B) methodology [13] and provides a comparison to the dissolution behaviour of standard MW25 glass – the UK's traditional HLW (without ZnO and CaO content), which has been previously reported in the literature.

EXPERIMENTAL DETAILS

CaZn MW28 was fabricated on the vitrification test rig (VTR) at the Sellafield Ltd. site, where the average internal temperature at the time of pouring was 1028 °C. The analysed composition, incorporating 28 wt.% oxide (o) and Magnox (m) blend waste at a ratio of 50o:50m was: 5.6 Al_2O_3, 16.3 B_2O_3, 1.0 BaO, 4.6 CaO, 1.5 CeO_2, 0.7 Cr_2O_3, 1.7 Cs_2O, 3.2 Fe_2O_3, 1.9 Gd_2O_3, 0.9 La_2O_3, 3.0 Li_2O, 2.9 MgO, 2.3 MoO_3, 6.9 Na_2O, 2.4 Nd_2O_3, 0.5 NiO, 0.7 Pr_2O_3, 0.6 RuO_2, 34.4 SiO_2, 0.6 Sm_2O_3, 0.5 SrO, 0.3 TeO_3, 0.3 Y_2O_3, 4.4 ZnO and 2.6 ZrO wt.%.

Crushed glass particles (75 – 150 µm diameter) were prepared [13] and PCT-B experiments were conducted at 90 °C in ultra-high-quality (UHQ) water (18.2 MΩ cm) (initial pH 7.2) at a surface area to volume ratio of 2,000 m^{-1}, for 112 days, under oxic conditions. A total of 1.1g of glass and 10 mL UHQ were used for each sacrificial test at time points 1, 3, 7, 14, 28, 35 and 112 d (in duplicate). The amount of glass dissolved was measured from the normalised mass loss of elements (*i*) (g m^{-2}) (NL_i) according to: $NL_i = (C_i - C_{i,b})/(f_i \times (SA/V))$, where; C_i and $C_{i,b}$ are the average concentration of *i* in the leachate and blank tests respectively (mg L^{-1}), measured using Inductively Coupled Plasma-Optical Emission Spectroscopy (ICP-OES, ThermoScientific iCAPDuo6300); f_i is the mass fraction of *i* (unitless) and SA/V is the surface area to volume ratio of the total particulates (m^{-1}), based on the geometric surface area. Uncertainty in NL_i was calculated by the standard deviation of the sum of uncorrelated random errors associated

with C_i, $C_{i,b}$, f_i and SA/V. Post-dissolution, altered particles were analysed in whole (without been ground and polished) by adhesion to carbon tabs and cross-sectioned from ground and polished epoxy mounts. Analysis was performed using scanning electron microscopy (SEM) and Energy Dispersive Spectroscopy (EDS) using a Hitachi TM3030 SEM (operating at an accelerating voltage of 15 kV) and a Bruker Quantax 70. X-ray diffraction (XRD) was performed on pristine and 35 d altered particles using a Bruker D2 Phaser X-ray Diffractometer, using Kα (λ = 1.541 Å) radiation generated from a Cu target at a working voltage of 30 kV and 10 mA. A Ni filter and a Lynx-Eye position sensitive detector were used. An angular range $10 < 2\Theta < 70$ with a 0.02^{o} step size of 0.17^{o} min^{-1} were used, with a total scan time of 110 minutes. The samples were rotated at frequency of 10 Hz. The geochemical modelling package PHREEQ-C version 3 was used to calculate the saturation indices of various secondary phases in leachates from 35 and 112 d time points. The concentration of elements from ICP-OES analysis were used as input, in addition to the initial and final pH to calculate a range of possible phases saturated in solution according to the Lawrence Livermore National Laboratory (LLNL) database.

RESULTS AND DISCUSSION

The NL_i for all elements are shown in Figure 1a, while Figure 1b compares the NL_B for CaZn MW28 with MW25. The measured pH values were consistent, between pH 9.6 and 9.8, and within instrumental error, throughout the experimental duration (Fig. 2).

The NL_{Si} for CaZn MW28 (Fig. 1a) showed an initial increase, followed by steady state dissolution, indicating that the residual rate (Stage II) had been achieved after 7 d. There was an increase in NL_i as a function of time for all elements throughout the experiment, with the exception of Mg, which decreased after 7 d, and Si, which decreased between 35 and 112 d. Additionally, Zn was only detected in solution after 112 d, which was just above quantification limits for ICP-OES. This suggests that these elements were either incorporated into the silica gel layer at the surface of the glass, or formed Mg- and Zn-bearing silicate precipitates. Concurrent with the decrease in NL_{Mg} (at 7 d), there was a nearly linear increase in the NL_B, which continued until the end of the experiment (Fig. 1b). Such behaviour is termed “rate resumption” (Stage III) in the glass dissolution literature.

Secondary silicate phases containing Mg and Zn were not identified in the XRD traces (Fig. 3) post 35 d. The Mg- and Zn-containing phyllosilicate smectite clays, saponite ($Ca_{0.2}Mg_3(Si,Al)_4O_{10}(OH)_2 \cdot 4H_2O$) and sauconite ($Na_{0.3}Zn_3(Si, Al)_4O_{10}(OH)_2 \cdot nH_2O$ [5] are potentially expected to form by 112 d. The precipitation of such clays is suggested to be responsible for the increase in dissolution from 7 – 112 d. XRD also potentially identified the following crystalline phases in the pristine glass: RuO_2; Fe_3O_4; CeO_2; and $Nd_2Zr_2O_7$.

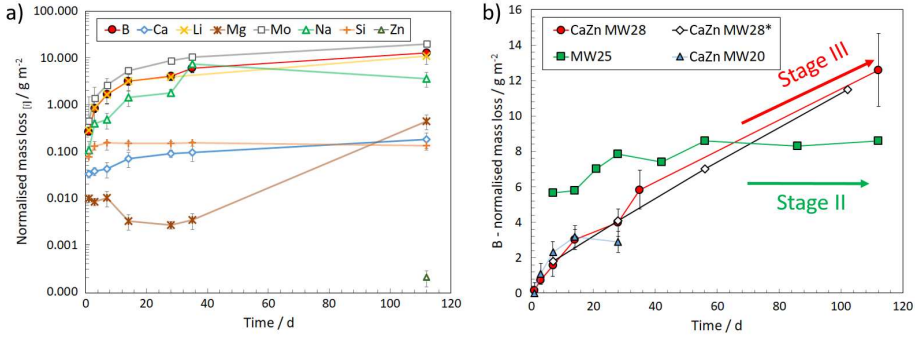

Figure 1. a) Normalised mass loss of elements [i] from CaZn MW28 post 112 d PCT-B leaching at 90 °C in UHQ water; b) comparison of NL_B from CaZn MW28 with the literature – CaZn MW28* [1], CaZn MW20 [12] and MW25 [14].

EDS analysis and BSE-SEM images revealed the presence of an alteration layer approximately 4 µm thick, which was overlaid by secondary precipitates and a potential smectite clay layer (Fig. 4). The identification of smectite clays was based on the presence of a similar morphology ("fuzzy blanket") to the clays identified by Muller *et al.* [11] and tentatively by a slight Mg-enrichment at the edge of the altered layer in the EDS map.

These observations were consistent with PHREEQ-C geochemical modelling, which predicted the formation of saponite at 35 and 112 d, and Zn_2SiO_4 after 112 d. Zinc was detected in solution after 112 d only, which does not rule out the potential for Zn_2SiO_4 to form on the surface/in the silica gel layer prior to 112 d. Note that sauconite was not available as a phase in the thermodynamic database utilised, therefore was not predicted to form. The Ca-containing zeolites mesolite ($Na_{.676}Ca_{.657}Al_{1.99}Si_{3.01}O_{10}{\cdot}2.647H_2O$) and scolecite ($CaAl_2Si_3O_{10}{\cdot}3H_2O$) were also predicted to be saturated in solution after 35 and 112 d. The NL_{Mg} increased between 35 - 112 d, possibly due to the dissolution of Mg-containing secondary phases. Future work using micro-focus XRD may confirm the identification of such phases.

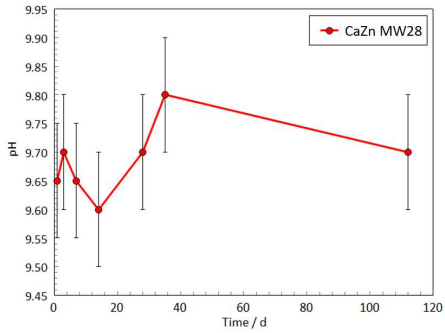

Figure 2. The pH measurements of the leachate from CaZn MW28 during 112 d PCT-B leaching at 90 °C in UHQ water.

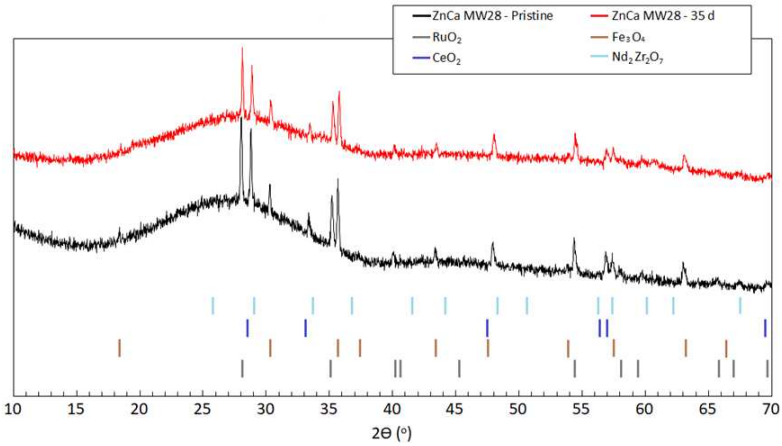

Figure 3. XRD traces of CaZn MW28 pristine (black trace) and post 35 d PCT-B leaching at 90 °C in UHQ water (red trace).

The NL_B for CaZn MW28 obtained in the present study and in that of Harrison and Brown [1], was compared with that of MW25 (which does not include ZnO and CaO) obtained by Harrison [14], under identical dissolution conditions, as shown in Figure 1b. It is clear that, at greater reaction progress (> 50 days), MW25 is more chemically resistant to dissolution. Furthermore, the mechanism of dissolution appears to be different when ZnO and CaO are added to the glass: for MW25 the dissolution behaviour appears to reach stage (II) dissolution, while CaZn MW glasses display stage (III)-type behaviour over the same duration of leaching.

One reason for the difference could be attributed to different pH values imposed by each glass, although a direct comparison of CaZn MW28 with MW25 from Harrison [1] is not possible since the pH values in that study were not published. However, a comparison with the study of Curti *et al*. [15], under similar test conditions (SA/V = 1,200 m^{-1} and an MW-type glass with approximately 22-28 wt.% waste loading) showed that the same pH was obtained for the MW-type glass as CaZn MW28 studied here (CaZn MW28 measured pH_{RT} 9.7 after 112 d and MW-type measured pH_{RT} 9.6 and $pH_{90\ C}$ 9.1 after 4,500 d). Hence, the difference in the dissolution behaviour may be due to: 1) the potential precipitation of Zn-bearing secondary phases or 2) the combined effect of Mg- and Zn-bearing silicate precipitates [16-18], which consume Si, limiting the formation of a protective altered gel layer. Note that the Mg content was 2.9 and 1.2 wt. % for CaZn MW28 and MW25, respectively. Mg-bearing saponite clay was abundantly formed on the MW-type glass containing 5.9 wt.% MgO studied by Curti *et al*. [15], whereby dissolution was sustained at a low residual rate (stage II), with a $NL_B \sim 13$ / g m^2 after 4,500 d in contrast to CaZn MW28, which measured $NL_B = 12.7$ / g m^2 after 112 d. This suggests that the precipitation of Zn-bearing silicate phases is a more predominant factor in dissolution rate enhancement. There was a combined concentration of 7.3 wt. % ZnO and MgO in CaZn MW28.

The behaviour of CaZn MW28 is consistent with the experiments performed by Harrsion and Brown [1] on the same glass, and with Zhang *et al.* [12] who used a similar composition, but which did not contain Al and had a lower waste incorporation (20 wt. %) - CaZn MW20 (Fig. 1b). These data are in agreement with studies on simplified borosilicate glasses containing Zn. For example Gin *et al.* [5] observed constant aggressive stage II dissolution (and the precipitation of sauconite) throughout a 1,700 d test on a simple 4-component formulation ($13.8Na_2O{\cdot}2.7ZnO{\cdot}13.8B_2O_3{\cdot}65.9SiO_2$ wt. %) under similar experimental conditions (however, no NL_B was reported so these values cannot be compared).

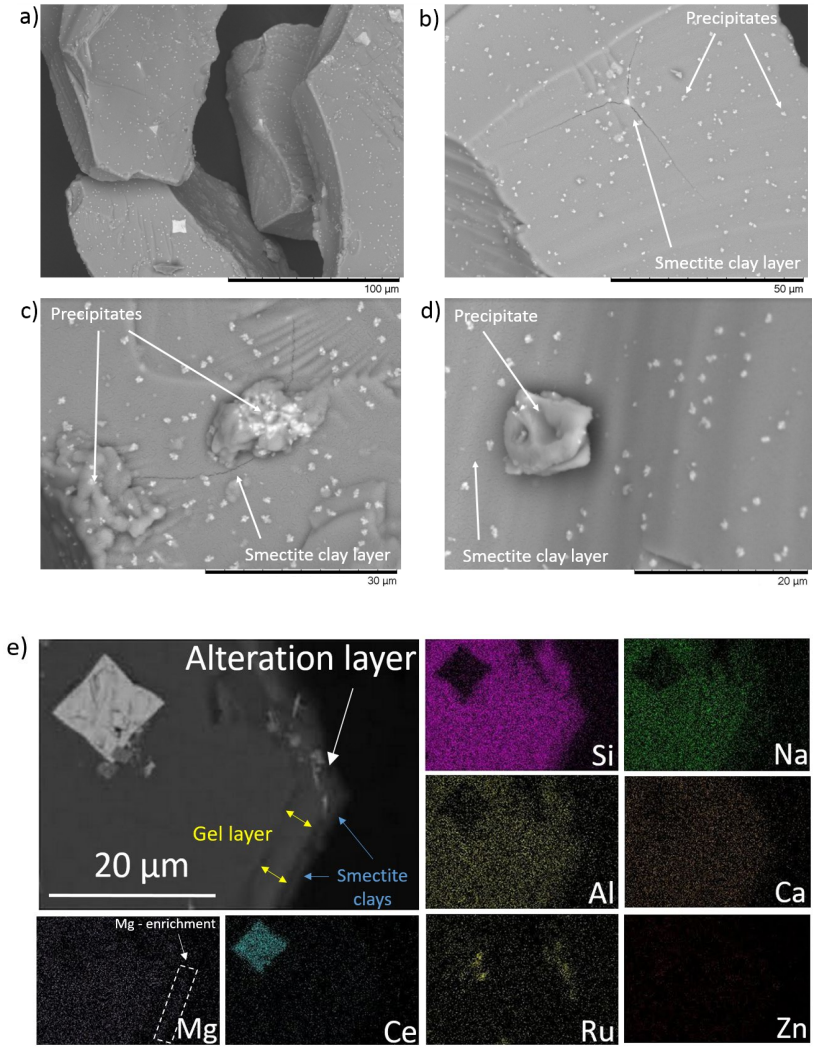

Figure 4. (a – d) BSE-SEM images of CaZn MW28 post 35 day PCT-B leaching at 90 °C in UHQ water. Note the "fuzzy blanket" smectite clay layer and (e) cross sectioned elemental mapping displaying a tentative Mg-enriched altered layer.

CONCLUSIONS

This investigation highlighted that the dissolution rate of MW-type simulant HLW glasses was increased by the addition of ZnO and CaO, when PCT-B experiments were performed for 112 d PCT-B at 90 °C in UHQ water. The formation of Mg- and Zn-smectite clays (potentially saponite and saucontite, respectively) may play a role in driving the dissolution rate to stage III, highlighting the detrimental effect of the incorporation of Mg and Zn (7.3 wt. % combined) in the waste glass on the dissolution at greater reactive progress.

ACKNOWLEDGMENTS

This work was funded, in part, by the EPSRC Next Generation Nuclear Centre for Doctoral Training Centre under grant EP/L015390/1. Financial support for CLC from the EPSRC (ECR Fellowship; EP/N017374/1) is acknowledged. This research was performed at the MIDAS Facility, at the University of Sheffield, which was established with support from the UK Department of Energy and Climate Change.

REFERENCES

[1] M. T. Harrison and G. C. Brown. *Mat. Let.* **221**, 154-156 (2018).
[2] B. F. Dunnett, N. R. Gribble, R. Short and E. Turner. *Glass. Tech.: Eur. J. Glass Sci. Tech.* **53** (4), 166-171 (2012).
[3] R. Short. *Proc. Mater. Sci.* **7**, 93-100 (2014).
[4] Matlack *et al. Sci. Bas. Nuc. Was. Man. XXII*, Paper 9.55, Mater. Res. Soc. Fall Meeting (1998).
[5] S. Gin, P. Frugier, P. Jollivert, F. Brugier and E. Curti. *Int. J. App. Gla. Sci*. **4**, [4], 371-382 (2013).
[6] C. M. Jantzen, W. E. Lee and M. I. Ojovan, "Radioactive waste conditioning, immobilisation, and encapsulation processes and technologies: Overview and advances," In *Radioactive waste management and contaminated site clean-up: Processes, technologies and international experiences,* W. E. Lee, M. I. Ojovan and C. M. Jantzen, Eds. Cambridge: Woodhead, 2013, pp. 171-272 (2013).
[7] C. A. Utton, R. J. Hand, P. A. Bingham, N. C. Hyatt, S. W. Swanton and S. J. Williams. *J.Nuc.Mat.* **435**, 112-122, (2013).
[8] H. Aréna. D. Rébiscoul, R. Podor, E. Garcès, M. Cabie, J. –P. Mestre and N. Godon. *Geo. et Cos. Acta.* **239**, 420-445 (2018).
[9] T. Chave, P. Frugier, S. Gin and A. Ayral. *Geo.Chim.Act*. **75**, 4125-4139, (2011).
[10] C. L. Corkhill, N. J. Cassingham, P. G. Heath and N. C. Hyatt. *Int. J. App. Gla. Sci*. **4**, [4], 341-356 (2013).
[11] I. S. Muller, S. Ribet, I. Pegg, S. Gin and P. Frugier. *Cer. Trans.* **176**, 191-199, (2006).
[12] H. Zhang, C. L. Corkhill, P. G. Heath, R. J. Hand, M. C. Stennett, N. C. Hyatt. *J. Nuc. Mat.* **462,** 321-328 (2015).
[13] ASTM C1285-14, Standard Test Methods for Determining Chemical Durability of Nuclear, Hazardous, and Mixed Waste Glasses and Multiphase Glass Ceramics: The Product Consistency Test (PCT), ASTM International, West Conshohocken, PA, (2014).
[14] M.T. Harrison. *Proc. Mat. Sci.* **7**, 186-192 (2014).
[15] E. Curti, J. L. Crovisier, G. Morvan and Am. M. Karpoff. *App. Geochem.* **21**, 1152-1168 (2006).
[16] B. M. J. Thien, N. Godon, A. Ballestero, S. Gin and A. Ayral. *J.Nuc.Mat.* **427**, 297-310, (2012).
[17] B. Fleury, N. Godon, A. Ayral and S. Gin. *J.Nuc.Mat.* **442**, 17-28, (2013).
[18] H. Aréna, N. Godon, D. Rébiscoul, R. Podor, E. Garcès, M. Cabie and J.–P. Mestre. *J.Nuc.Mat.* **470**, 55-67, (2016).